Numerical modeling of Converging Compound Channel Flow

B. Naik[1], P. Singh[2], K.K.Khatua[3]

1 Ph. D. Research Scholar, Department of Civil Engineering, National Institute of Technology Rourkela, India. Email:banditanaik1982@gmail.com
2 M.Tech Scholar, Department of Civil Engineering, National Institute of Technology Rourkela, India. Email:prateek.k.singh1992@gmail.com
3 Associate Professor, Department of Civil Engineering, National Institute of Technology Rourkela, India. Email: kkkhatua@yahoo.com

Abstract

This paper presents numerical analysis for prediction of depth-averaged velocity distribution of compound channels with converging flood plains. Firstly, a 3D Computational Fluid Dynamics (CFD) model is used to establish the basic database under various working conditions. Numerical simulation in two phases is performed using the ANSYS-Fluent software. *k-ω* turbulence model is executed to solve the basic governing equations. The results have been compared with high quality flume measurements obtained from different converging compound channels in order to investigate the numerical accuracy. Then ANN (Artificial Neural Network) are trained based on the Back Propagation Neural Network (BPNN) technique for depth-averaged velocity prediction in different converging sections and these test results are compared with each other and with actual data. The study has focused on the ability of the software to correctly predict the complex flow phenomena that occur in channel flows.

Keywords: *compound channel, stage discharge, Prismatic, non-prismatic, ANN, ANSYS*

1 INTRODUCTION

Distribution of depth-averaged velocity is important aspect in river hydraulics and engineering problems in order to give a basic understanding of the resistance relationship, to understand the mechanisms of sediment transport and to design sustainable channels etc. Due to continuous settlement of people near the riverbank and due to natural causes, the channel with floodplain cross-sections behaves as converging type non-prismatic compound channels. An improper estimation of floods in these regions, will lead to an increase in the loss of life and property. A number of authors [1-8] has investigated the depth-averaged velocity distribution and flow resistance in prismatic compound cross-sections. These models are not appropriate to predictions in compound channels with converging flood plain because of non-uniform flow occurs from section to section. Therefore, there is a need to evaluate the depth-averaged velocity in the main channel and floodplain at various locations of a converging compound channel. Converging channel flows, being highly complicated, are a matter of recent and continued research. For a better understanding of the structure of turbulent flow in converging compound channels, it is necessary to undertake detailed measurements. Because of the difficulty in obtaining sufficiently accurate and comprehensive field measurements of velocity and shear stress in converging compound channels under non-uniform flow conditions, considerable reliance must still be placed on well focused laboratory investigations under steady flow conditions to provide the

information concerning the details of the flow structures and lateral momentum transfer. Attention must be paid to the fact that physical models are very expensive, especially when a large number of influencing parameters have to be studied. Sometimes, it is impossible to construct a physical model for certain prototypes. Therefore, there is urgent need for economic mathematical prediction models. In past a lot of experimental research has been done on prismatic compound channel flows but relatively less usage has been made of numerical techniques on non-prismatic compound sections. After the development of powerful computers and sophisticated CFD (Computational Fluid Dynamics) techniques, much research is now being conducted using these techniques in different research areas. This is not only due to economy and less time required with CFD methodology but also due to the fact that through CFD one can cover those aspects of flow behavior which are very difficult to observe through experimentation. In recent years, numerical modeling of open channel flows has successfully reproduced experimental results. Computational fluid dynamics (CFD) has been used to model open channel flows ranging from main channels to flood plains. Simulations have been performed by Krishnappan & Lau (1986), Kawahara & Tamai (1988) and Cokljat (1993). CFD has also been used to model flow features in natural rivers by Sinha et al. (1998), Lane et al. (1999), and Morvan (2001). Hodskinson (1996, 1998) was one of the first to present results using a commercial CFD. In this case FLUENT was used to predict the 3D flow structure in a 90-degree bend on the River Dean in Cheshire. Pan & Banerjee (1995), Hodges & Street (1999), and Nakayama & Yokojima (2002) studied free surface fluctuations in open channel flow by employing the LES method. Hsu *et al*. (2000) have reported the existence of the inner secondary currents in the rectangular open-channels, which occur at the junction of the free surface and sidewall. Knight *et al*. (2005) applied state-of-the-art CFD software to explore the physics within open-channel flows. In their research work they applied three different turbulent models, namely the k-ϵ, Reynolds Stress model by Speziale, Sarkar and Gatski (SSG) by Speziale *et al*. (1991) and Reynolds Stress ω or SMC-ω (implemented in ANSYS-CFX) models to trapezoidal channel. Thomas and Williams (1995a) and Cater and Williams (2008) simulated an asymmetric rectangular compound channel using LES for a relative depth of $\beta = 0.5$. They have predicted mean stream wise velocity distribution, secondary currents, bed shear stress distribution, turbulence intensities, TKE, and calculated lateral distribution of apparent shear stress. Gandhi et al. (2010) determined the velocity profiles in two directions under different real flow field conditions and also investigated the effects of bed slope, upstream bend and a convergence / divergence of channel width. Kara *et al*. (2012) compared the depth-averaged stream wise velocities obtained by LES with calculated by analytical solution of Shiono and Knight Method (SKM), and concluded that the analytical approach to their problem requires calibration of the lateral eddy viscosity coefficient, λ, and the secondary current parameter, Γ. Xie *et al*. (2013) used LES to simulate asymmetric rectangular compound channel. In this study the distributions of the mean velocity and secondary flows, boundary shear stress, turbulence intensities, TKE and Reynolds stresses were in a good agreement with the experimental data. Filonovich (2015) used ANSYS-CFX package to allow the simulation of uniform flows in straight asymmetric trapezoidal and rectangular compound channels with several different RANS turbulence closure models.

In the last decade machine-learning methods were the subject of many researches in engineering problems and also in water resources engineering (Cheng et al., 2002; Lin et al., 2006; Muzzammil, 2008; Wang et al., 2009; Wu et al. 2009; Ghosh et al., 2010; Safikhani et al.,

2011). Bilgil and Altun (2008) predicted friction factor in smooth open channel flow using ANN. Sahu et al. (2011) proposed an artificial neural network model for accurate estimation of discharge in compound channel flume and Moharana and Khatua (2014) studied the flow resistance in meandering compound channels by using ANFIS. Abdeen (2008) adopted an ANN technique to simulate the impacts of vegetation density, flow discharge and the operation of distributaries on the water surface profile of open channels. Yuhong and Wenxin (2009) studied the application of ANN for prediction of friction factor of open channel flows. The ANN technique has also been successfully applied to compound open channel flow for the prediction of the hydraulics characteristics, such as integrated discharge and stage-discharge relations (Bhattacharya & Solomatine 2005; Jain 2008; Unal et al. 2010; Sahu et al.2011)

In the first part of this paper, 3D numerical simulations of flow field with two phases (water & air) are carried out with the software ANSYS FLUENT to study the variation of velocity profiles in different converging sections of a compound channel. In multiphase fluid flow, a phase is described as a particular class of material that has a certain inertial response and interaction with the fluid flow and the potential field in which it is immersed. Currently there are two approaches for the numerical calculation of multiphase flows: The Euler-Lagrange approach and the Euler-Euler approach. Even though air is considered as a secondary material we have taken it in analysis to give it more real time analogy, by compromising over the computational time.
In order to solve turbulence equations, the k-ω model is used since more accurate near wall treatment with automatic switch from wall function to a low Reynolds number formulation based on grid spacing. Numerical results are verified using experimental data obtained in an experimental analysis in the Hydraulics and Fluid Mechanics Laboratory of the Civil Engineering Department of NIT, Rourkela. This study shows that the numerical model results have good agreement with experimental ones. There are always some limitations in experimental studies and obtaining experimental data in every point of a channel is not easy. Also after doing an experimental test and obtaining the velocity in the desired point, measuring the velocity in other points needs to do the experimental test again. Artificial intelligence is evaluated here as a solution to this problem. By training an ANN based on experimental data of the points that are available, the ANN assists investigators in calculating the velocity at other points of the channel with good accuracy. This paper employs ANN for the prediction of depth average velocity of converging compound channel, after using the computational fluid dynamics (CFD) technique to establish the basic database under various working conditions. Quite a few model available for prediction of depth average velocity usually under performs when the meagre datasets are used for estimation. Generally, this happens while predicting the depth average velocity for a wide range of hydraulic conditions and geometries of compound channel. To alleviate the above problem, a robust prediction strategy based on an ANN has been proposed. It is demonstrated that the ANN model is quite capable of predicting a depth average velocity with reasonable accuracy for a wide range of hydraulic conditions.

2 EXPERIMENTAL WORKS

Experiments have been conducted at the Hydraulics and Fluid mechanics Laboratory of Civil Engineering Department of National Institute of Technology, Rourkela, India. Three sets of non-prismatic compound channels with varying cross section were built inside a concrete flume with Perspex sheet measuring 15m long × 0.90m width × 0.5m depth. The width ratio (α = flood plain width (B)/main channel width (b)) of the channel was 1.8 and the aspect ratio (δ = main channel

width (b)/main channel depth (h)) was 5. Keeping the geometry constant, the converging angles of the channels were varied as 12.38°, 9° and 5° respectively. Converging length of the channels fabricated were found to be 0.84m, 1.26m and 2.28m respectively. Longitudinal bed slope of the channel was measured to be 0.0011, satisfying subcritical flow conditions at all the sections of the non-prismatic compound channels. Roughness of both floodplain and main channel were kept smooth with the Manning's *n* 0.011 determined from the inbank experimental runs in the channel. The flow conditions in all sections were turbulent. A re-circulating system of water supply was established with pumping of water from the large underground sump located in the laboratory to an overhead tank from where water flows under gravity to the experimental channels. Adjustable vertical gates along with flow strengtheners were provided in the upstream section sufficiently ahead of rectangular notch to reduce turbulence and velocity of approach in the flow near the notch section. An adjustable tailgate at the downstream end of the flume helps to maintain uniform flow over the test reach. Water from the channel was collected in a volumetric tank of fixed area that helps to measure the discharge rate by the time rise method. From the volumetric tank water runs back to the underground sump by the valve arrangement. For present work the experimental data Rezaei (2006) have been used. Rezaei (2006) have also used converging compound channels of angles 11.31^{0}, 3.81^{0}, 1.91^{0} giving the same subcritical flow and smooth surfaces. They have found the depth-averaged velocity and boundary shear distribution of the same channels under different flow conditions. Figure 1(a) shows the plan view of experimental setup. Figure 1(b) shows the plan view of different test reach with cross-sectional dimensions of both NITR & Rezaei (2006) channels. Figure 1(c) shows the typical grid showing the arrangement of velocity measurement points along horizontal and vertical direction in the test section.

A movable bridge was provided across the flume for both span-wise and stream-wise movements over the channel area so that each location on the plan of compound channel could be accessed for taking measurements. Water surface depths were measured directly with a point gauge located on an instrument carriage. The flow depth measurements were taken along the center of the flume at an interval of 0.5 m both in upstream and downstream prismatic parts of flume and at every 0.1 m in the converging part of the flume. A micro-Pitot tube of 4.77 mm external diameter in conjunction with suitable inclined manometer and a 16-Mhz Micro ADV (Acoustic Doppler Velocity-meter) was used to measure velocity at these points of the flow-grid. In some points, micro-ADV cannot take the velocity reading (up to 50cm from the water surface).In such points Pitot tube was used to take the velocity. The Pitot tube was physically rotated with respect to the main stream direction until it gave maximum deflection of the manometer reading. A flow direction finder having a minimum count of 0.1° was used to get the direction of maximum velocity with respect to the longitudinal flow direction. The angle of limb of Pitot tube with longitudinal direction of the channel was noted by the circular scale and pointer arrangement attached to the flow direction meter. The overall discharge obtained from integrating the longitudinal velocity plot and from volumetric tank collection was found to be within ±3% of the observed values. Using the velocity data, the boundary shear at various points on the channel beds and walls were evaluated from a semi log plot of velocity distribution.

3 NUMERICAL MODELING

A number of CFD packages (Fluent, CFX, Star-CD, and others) are now available and have been used for research in water flows Van Hoffa et al. (2010). In recent past, a good number of researchers have used these software packages for prediction of different aspects of 3D flow fields e.g Sahu et al. (2011). They detected that flow features in compound channels are dependent on topography of the channel, surface roughness etc. However, the flow behavior changes are still an unresolved phenomenon and attempts are underway to address this problem. These researchers attempted to predict the flow behavior using different numerical models as it is difficult to capture all flow features experimentally but still a lot of work is to be done. This is due to various problems which are encountered in numerical modelling such as grid generation, choice of turbulence model, discretization scheme, specifying the boundary and initial conditions etc.

In this work, an attempt has been made to improve the understanding of 3D flows in converging compound channels. For this purpose, a 3D numerical code FLUENT has been tested for its suitability for simulation of flood flows. Initially, the closure problem of governing equations was considered as there is no universal closure model which is acceptable for all flow problems. Each has its own advantages and disadvantages. Therefore, some consideration must be taken when choosing a turbulence model including, physics encompassed in the flow, level of accuracy and computation resources available one has to attempt different models and then to choose the one producing best results. The models tested here were standard k-ε, LES and k-ω. The one with best output (standard k-ω in this case) was then used for all simulation works. The k-ω model is chosen on the basis of the computational time and resource availability. Beside the fact that k-ϵ more or less produce same results as that of the k-ω model but the other two-equation model 'k-ω' performs better near the wall region and k-ϵ performs better in the fully turbulent region (Filonovich 2015). On the other hand, LES partially resolves the turbulence and give good results when compared to experimental data (Kara et al. 2012). The overall idea of modelling through sub grid model for small time and length scale (Kolmogorov scales i.e. ratio of small eddies to large eddies lengthwise as well as time wise) and resolving the large scale through governing equation needs an exceptionally high computation effort. To optimize such computational resource and time requirement, k-ω model is chosen even though compromises are made over the results which are acceptable than spending high in computational resources and time. It was used for prediction of resultant velocity contours on free surface, pressure, turbulence intensity and secondary flow velocities at different sections along the converging length.

Generally FLUENT involves three stage. The first stage is the pre-processing, which involve geometry creation, setting of grid and defining the physics of the problem. The second stage involves the application of solver to generate a numerical solution. In the third stage post-processing takes place, where the results are visualized and analyzed.

3.1 Geometry

The first step in CFD analysis is the explanation and creation of computational geometry of the fluid flow region. A consistent frame of reference for coordinate axis was adopted for creation of geometry. Here in coordinate system, x axis corresponded the lateral direction which indicates the width of channel bed. Y axis aligned stream-wise direction of fluid flow and Z axis represented the vertical component or aligned with depth of water in the channel. The origin was placed at the upstream boundary and coincided with the base of the center line of the channel.

The water flowed along the positive direction of the y-axis. The simulation was done on a non-prismatic compound channel with a converging flood plain. The setup of the compound channel is shown in Figure 2.
For identify the domain six different surfaces are generated. Figure 3 shows the different Geometrical entities used in a non-prismatic compound channel

- Inlet
- Outlet
- Free Surface
- Side Wall
- Channel Bottom
- Centre line

3.2 Mesh generation

The second and very important step in numerical analysis is setting up the discretized grid associated with the geometry. Construction of the mesh involves discretizing or subdividing the geometry into the cells or elements at which the variables will be computed numerically. By using the Cartesian co-ordinate system, the fluid flow governing equations i.e. momentum equation, continuity equation are solved based on the discretization of domain. The meshing divides the continuum into a finite number of nodes. Generally, one of three different methods, i.e. Finite Element, Finite Volume and Finite Difference, can discretize the equations. Fluent uses Finite Element (FE) based Finite Volume Method (FVM). This alternative uses the control volume analysis, which is vertex-centered, i.e. the solution correlation variables are saved at the nodes (vertices) of the mesh. The concept of FVM is used to convert the partial differential equation into system of algebraic equation, which can be solved through closure. Two prominent discretization steps involved at this stage are discretization of the computational domain and discretization of the equation. The discretization of the computational domain is done through mesh generation, which can be identified later through control volume constructions. However, a very dense mesh of nodes causes excess computational time and memory. For CFD analysis, more nodes are required in some areas of interest, such as near wall and wake regions, in order to capture the large variation of fluid properties. Thus, the structure of grid lines causes further unnecessary use of computer storage due to further refinement of mesh. In this study, the flow domain is discretized using an unstructured grid and body-fitted coordinates. Unstructured grid is used so that intricacies can be covered under the grid which is left over in structured one. The detailed meshing of the flow domain is shown in Figure 4.

3.3 Solver setting

3.3.1 Setup

After the meshing part is completed, various inputs are given in the Setup section. **VOF** (volume of fluid) model is the only model available for open channel flow simulation in ANSYS-FLUENT, which is based on the idea of volume fraction (Hirt and Nichols 1981). In this method, a transport equation is solved for the volume fraction at each time step whereupon the shape of the free surface is reconstructed explicitly using the distribution of the volume fraction function. The “reconstruction” of the free surface can be explained more clearly through the concept of water volume fraction. Free surface is defined as the cell, which takes the value of the water

volume fraction as non-zero while a zero value indicates that no fluid is present in the cell. The value of 0.5 for the water volume fraction is indicative of the fact that free surface position is detected. This method can define sharp interfaces and is robust. VOF is capable of calculating time dependent solutions. Flow in an open channel is generally bound by channel from all directions except for the upward free surface. To achieve a free surface zero friction interface, a command called "surface_symmetry" is given in named selection. Velocity inlet for inlet and pressure outlet for outlet is defined and the roughness coefficient is added to the walls for "no slip" condition. Transient flow was chosen because the flow parameters were varied in time in the experiment. Gravity is check marked and the value for Z-axis is given as -9.81 because gravity acts downward opposite to the z-direction vector. As mentioned earlier, the turbulence model was chosen as k- ω model. PISO was selected for solving the pressure equation, as it is generally a pressure-based segregated algorithm recommended for transient flow conditions (Issa 1986). Also, PISO scheme may aid in accelerating convergence for many unsteady flows. Finally, solver is patched and run to apply all the settings as well as conditions mentioned above. It's just finalizing and complying the settings. The equation solved in the CFD are usually iterative and starting from initial approximation, they iterate to a final result. However, these iterations are terminated at some step to minimize the numerical effort. This termination are done on the basis of normalized residual target which is by default is set to 10^{-4}, which leads to loose convergence target. For problems like compound channel in order to obtain more accuracy residual target should be placed a value near around 10^{-6}. Time step size was set to 0.001s and number of iteration given was 1000 for better accuracy and convergence of the iteration. Time step size, Δt, is then set in the Iterate panel, Δt must be small enough to resolve time-dependent features; making sure that the convergence is reached within the number of max iterations per time step. The order of magnitude of an appropriate time step size can be estimated as ratio of typical cell size to the characteristic flow velocity. Time step size estimate can also be chosen so that the unsteady characteristics of the flow can be resolved (e.g. flow within a known period of fluctuations). To iterate without advancing in time, use zero time steps.

3.3.2 Governing Equations

ANSYS Fluent uses the finite volume method to solve the governing equations for a fluid. It provides the capability to use different physical models such as incompressible or compressible, inviscid or viscous, laminar or turbulent etc. The most practical and still the most popular method of dealing with turbulence is that based on the RANS method. With this method, all scales of turbulence are modelled. Several models were studied to compare the effect of turbulent modeling in the converging compound channel, including the following: (1) k-Epsilon, (2) *k-ω* and (3) Large Eddy Simulation (LES) model. Here k-*ω* model is used for turbulence modeling. The *k-ω* model solves the *k*-transport equation and a transport equation for *ω*. The *k*-transport equation and the transport equation for *ω* can be written (Wilcox 1988)

$$\frac{\partial k}{\partial t} + U_i \frac{\partial k}{\partial x_i} = \frac{\partial}{\partial x_i}\left(\frac{v_t}{\sigma_k}\frac{\partial k}{\partial x_i}\right) + P - \beta' k\omega \quad (1)$$

$$\frac{\partial \omega}{\partial t} + U_i \frac{\partial k}{\partial x_i} = \frac{\partial}{\partial x_i}\left(\frac{v_t}{\sigma_\omega}\frac{\partial k}{\partial x_i}\right) + \alpha \frac{\omega}{k} P - \beta \omega^2 \quad (2)$$

and the eddy viscosity is given by

$$v_t = k/\omega \quad (3)$$

P is the turbulence kinetic energy production rate. Menter [49] as suggested the turbulence equation:

$$P = \min (P, 10\beta' k\omega) \quad (4)$$

It represents the rate at which the energy is fed from the mean flow to each stress component. The estimation of the production term can be done directly from the stress and the men flow strain rate components and thus needs no modelling other than this all other terms need modelling.

The *k-ω* model involves five empirical constants *β', β, α, σ_k and σ_ω*. They have their universal constant values, which have been derived on the basis of high quality data. Their values vary from one turbulence model to another. For any particular turbulence model, the values of these constants remain same for all simulation purposes. For standard *k-ω*, their values are presented in Table 2.

3.3.3 Boundary conditions

Four different types of boundary condition were considered in this study. These are (i) inlet, (ii) outlet, (iii) water surface, and (iv) walls of the geometry

(i) Inlet

The velocity distribution at the upstream cross-section was taken as inlet boundary condition. At the inlet, turbulence properties i.e. k (turbulence kinetic energy) and (*ω* turbulence dissipation rate) must be specified. These were calculated as [28]

$$k = IU^2 \quad (5)$$

$$\omega = \frac{k^{1/2}}{l} \quad (6)$$

Where I is the turbulence intensity and U is the mean value of stream-wise velocity. l is the turbulence length scale

(ii) Outlet

At the outlet, the pressure condition was given as the boundary condition and pressure was fixed at zero. Importance of the outflow boundary at an appropriate location can be explained through the influence of the downstream condition. Thus it makes extremely imperative to put the downstream end far enough to prevail the fully developed state.

(iii) Channel and Floodplain Boundaries

A no-slip boundary condition was considered at the walls. This means that the velocity components should be zero at the walls. The no-slip condition is the default, and it indicates that the fluid sticks to the wall and moves with the same velocity as the wall, if it is moving. The wall is the most common boundary condition in bounded fluid flow problem. Setting the velocity near wall as zero under no-slip condition is appropriate condition for the solid boundary. The wall boundary condition in the turbulent flow is implemented and initiated by evaluating the dimensionless distance 'z^+' from the wall to the nearest boundary node. This dimensionless distance is the function of the near wall node to the solid boundary, friction velocity and the kinematic viscosity. The near wall treatment will depend on the position of the nearest to the

boundary node. If $z^+ \leq 11.06$ the nearest to boundary node will lie in the viscous sub-laminar layer where profile is linear and very fine meshing is required. This will tend to intensify the computation effort, which is being dedicated for near wall treatment. In another case where $z^+ > 11.06$ the nearest boundary node will lie in the buffer layer which is the transition region from viscous sublayer and the log law region. The main shortcoming of the wall function approach is their dependability on the nearest node distance from the wall, which cannot be overcome through refining since it does not guarantees high accuracy. Nevertheless, the problem of discrepancy in the wall function approach can be subsidized through Scalable wall function where limiting the z^+ value to not fall below 11.06 (the intersection of linear profile and log-law) is concentrated. Therefore, all mesh points are made lie outside the viscous sublayer and all fine mesh discrepancies are circumvented.

Thus, standard wall-function, which uses log-law of the wall to compute the wall shear stress is, used [50]. Fluid flows over rough surfaces are encountered in diverse situations. If the modeling is a turbulent wall-bounded flow in which the wall roughness effects are considered significant, it can include the wall roughness effects through the law-of-the-wall modified for roughness.

(*iv) Free Surface*

The water surface was defined as a plane of symmetry, which means that the normal velocity and normal gradients of all variables are zero at this plane. Free surface in the present study is modeled through VOF for estimating the domain for air and water (multiphase problem).

3.4 Results

A variety of flow characteristics can be considered in the post-processing software of CFD packages. This work has been concerned with the velocity distribution and the results are compared with experimental measurements. In general the user should make an attempt to validate the CFD results with known data so that there can be some confidence in the solution. In the case of open channel flow, the validation is most likely to take the form of a comparison against physical measurements and a qualitative understanding of what features should be present in the flow. As part of the analysis, the user may also wish to perform a sensitivity study and vary any parameters (such as roughness here) which have a degree of uncertainty, and determine what influence they have on the solution.

4. PREDICTION USING ANN

ANN is a new and rapidly growing computational technique and an alternative procedure to tackle complex problems. In recent years it has been broadly used in hydraulic engineering and water resources [36, 37]. It is a highly self-organized, self-adapted and self-trainable approximator with high associative memory and nonlinear mapping. ANNs may consist of multiple layers of nodes interconnected with other nodes in the same or different layers. Various layers are referred to as the input layer, the hidden layer and the output layer. The inputs and the inter-connected weights are processed by a weight summation function to produce a sum that is passed to a transfer function. The output of the transfer function is the output of the node. In this paper, multi-layer perception network is used. Input layer receives information from the external source and passes this information to the network for processing. Hidden layer receives

information from the input layer and does all the information processing, and output layer receives processed information from the network and sends the results out to an external receptor. The input signals are modified by interconnection weight, known as weight factor W_{ij} which represents the interconnection of i^{th} node of the first layer to the j^{th} node of the second layer. The sum of modified signals (total activation) is then modified by a sigmoidal transfer function (*f*). Similarly output signals of hidden layer are modified by interconnection weight (W_{ij}) of k^{th} node of output layer to the j^{th} node of the hidden layer. The sum modified *k* signal is then modified by a pure linear transfer function (*f*) and output is collected at output layer.

Let $I_p = (I_{p1}, I_{p2},\ldots,I_{pl}),\ p=1,2,\ldots,N$ be the p^{th} pattern among *N* input patterns. W_{ji} and W_{kj} are connection weights between i^{th} input neuron to j^{th} hidden neuron and j^{th} hidden neuron to k^{th} output neuron respectively.

Output from a neuron in the input layer is

$$O_{pi} = I_{pi},\ i=1, 2\ldots l \tag{7}$$

Output from a neuron in the hidden layer is

$$O_{pj} = f(NET_{pj}) = f\left(\sum_{i=0}^{l} W_{ji} O_{pi}\right),\ j = 1, 2.\ m \tag{8}$$

Output from a neuron in the hidden layer is

$$O_{pk} = f(NET_{pk}) = f\left(\sum_{i=0}^{l} W_{kj} O_{pj}\right),\ k=1, 2.\ n \tag{9}$$

4.1 Sigmoidal Function

A bounded, monotonic, non-decreasing, *S* Shaped function provides a graded non-linear response. It includes the logistic sigmoid function

$$F(x) = \frac{1}{1+e^{-x}} \tag{10}$$

Where *x* = input parameters taken

The architecture of back propagation neural network model, that is the *l-m-n* (*l* input neurons, *m* hidden neurons, and *n* output neurons) is shown in the fig.5

4.2 Learning or training in back propagation neural network

Batch mode type of supervised learning has been used in the present case in which interconnection weights are adjusted using delta rule algorithm after sending the entire training sample to the network. During training, the predicted output is compared with the desired output and the mean square error is calculated. If the mean square error is more, then a prescribed limiting value, it is back propagated from output to input and weights are further modified until the error or number of iteration is within a prescribed limit.

Mean Squared Error, E_p for pattern is defined as

$$E_p = \sum_{i=1}^{n} \frac{1}{2}\left(D_{pi} - O_{pi}\right)^2 \quad (11)$$

Where *Dpi* is the target output, O_{pi} is the computed output for the i^{th} pattern.

Weight changes at any time *t*, is given by

$$\Delta W(t) = -nE_p(t) + \alpha \times \Delta W(t-1) \quad (12)$$

n = learning rate i.e. $0 < n < 1$

α = momentum coefficient i.e. $0 < \alpha < 1$

4.3 Source of data

The data are collected from research work done in Hydraulic and Fluid Mechanics Laboratory, NIT Rourkela, [44] data, available at the laboratory of University of Birmingham, Wallingford and also generated data by using ANSYS-15 .The descriptions of geometrical parameters of above data are mentioned in Table.3.

4.4 Selection of hydraulic parameters

Flow hydraulics and momentum exchange in converging compound channels are significantly influenced by both geometrical and hydraulic variables, the computation become more complex when the floodplain width contracted and become zero. The flow factors responsible for the estimation of depth-averaged velocities are

(i) Converging angle denoted as θ

(ii) Width ratio (α) i.e .ratio of width of floodplain to width of main channel

(iii) Aspect ratio (σ) i.e. ratio of width of main channel (B) to depth of main channel (h)

(iv) Depth ratio (β) = (*H-h)/H,* where *H*=height of water at a particular section and, *h*= height of water in main channel

(v) Relative distance (X_r) i.e of point velocity in the length wise direction of the channel)/total length of the non-prismatic channel. Total five flow variables were chosen as input parameters and depth-averaged velocity as output parameter.

5. RESULTS

5.1 Results of ANSYS and CES

5.1.1 Verification

The values of depth-averaged velocity distributions of different cross-sections of the non-prismatic compound channel are achieved from the numerical models like CES (Conveyance Estimating System) and ANSYS then the results from the experimental data of both NITR and [44] channels were compared in Figures 6-11. As illustrated in Figures 6-10, the numerical model was in good agreement with experimental results but the results of the CES model have some differences with experimental results. The Conveyance and Afflux Estimation System (CES/AES) is a software tool for the improved estimation of flood and drainage water levels in rivers, watercourses and drainage channels. The software development followed recommendations by practitioners and academics in the UK Network on Conveyance in River Flood Plain Systems, following the Autumn 2000 floods, that operating authorities should make

better use of recent improved knowledge on conveyance and related flood (or drainage) level estimation. This led to a Targeted Program of Research aimed at improving conveyance estimation and integration with other research on afflux at bridges and structures at high flows. The CES/AES software tool aims to improve and assist with the estimation of:

- hydraulic roughness
- water levels (and corresponding channel and structure conveyance)
- flow (given slope)
- section-average and spatial velocities
- backwater profiles upstream of a known flow-head control e.g. weir (steady)
- afflux upstream of bridges and culverts
- uncertainty in accuracy of input data and output

Conveyance Estimation System (CES) is developed by joint Agency/DEFRA research program on flood defence, with contributions from the Scottish Executive and the Northern Ireland Rivers Agency, HR Wallingford. CES is based Reynolds-averaged Navier-Stokes (RANS) approach as the solution basis for estimation of conveyance. RANS equation of CES has been solved analytically by Shiono & Knight method. In this solution the converging fluid plain effect has not been considered which is reflected by the results of depth-averaged velocity and giving much error However, Fluent K-ω model take care of converging effect as well as interaction effect of geometry of converging compound channel.

5.2 Results of ANN

5.2.1 Testing of Back propagation neural network

Determination of depth-averaged velocity distribution of compound channel with converging flood plain is an important task for river engineer. Due to nonlinear relationship between the dependent and independent variables any model tools to provide the accurate depth-averaged velocity distribution. Numerical approach has also consumed more memory and time. So in the present work the ANN has been tested. The total experimental data set is divided into training set and testing set. For depth-averaged velocity calculations 32321 data are used among which 70% are training data and 30% are taken as testing data. The number of layers and neurons in the hidden layer are fixed through exhaustive experimentation when mean square error is minimised for training data set. It is observed that minimum error is obtained for 5-7-1 architecture. So the back propagation neural network (BPNN) used in this work has three layered feed forward architecture. The model was run on MATLAB commercial software dealing with trial and error procedure.

A regression curve is plotted between actual and predicted depth-averaged velocity of testing data which are shown in figure (12) .It can be observed that data are well fitted because a high degree of coefficient of determination R^2 of 0.91. Figure 13 shows the error histogram plot of the model.

6. ERROR ANALYSIS

To check the strength of the model, with the result from CES error analyses have been done. Mean Absolute Error (MAE), the Mean Absolute Percentage Error (MAPE), Mean Squared Error (MSE), the Root Mean Squared Error (RMSE) for all the converging compound channels for different geometry and flow conditions have been estimated. Efficiency criterion like R^2, Nash-Sutcliffe efficiency (E) have also been estimated to provide more information on the

systematic and dynamic errors present in the model simulation. The definitions of error terms are described below. The detailed results of the error analysis have been presented in table 4 .The expression used to estimate errors in different forms are

1. Mean Absolute Error (MAE)

The Mean Absolute Error has been evaluated as,

$$MAE = \frac{1}{n}\sum_i^n \left|\frac{P_i - O_i}{O_i}\right| \quad (13)$$

Where P_i=predicted values, O_i=observed values

2. Mean Absolute Percentage Error (MAPE)

Mean Absolute Percentage Error also known as Mean absolute Percentage Deviation. It was usually expressed as a percentage, and was defined by the formula

$$MAPE = \frac{1}{n}\sum_i^n \left|\frac{O_i - P_i}{O_i}\right| \quad (14)$$

3. Mean Squared Error (MSE)

Mean Squared Error measures the average of the squares of the errors. It is computed as

$$MSE = \frac{1}{n}\sum_i^n (P_i - O_i)^2 \quad (15)$$

4. Root Mean Squared Error (RMSE)

Root Mean Squared Error or Root Mean Squared Deviation is also a measure of the differences between values predicted by model or an estimator and the actually observed values. These individual differences are called as residuals when the calculations are performed over the data sample that is used for estimation, and are known as estimation errors when computed out of the sample. The RMSE is defined as

$$RMSE = \sqrt{MSE} \quad (16)$$

5. Coefficient of correlation R^2

The coefficient of correlation R^2 can be expressed as the squared ratio between the covariance and the multiplied standard deviations of the observed and predicted values. The range of R^2 lies between 0 and 1.0 which describes how much of the observed dispersion is explained by the prediction. A value of zero means no correlation at all whereas a value of 1 means that the dispersion of the prediction is equal to that of the observation.

6. Nash-Sutcliffe efficiency E

The efficiency E proposed by Nash and Sutcliffe [51] is defined as:

$$E = 1 - \frac{\sum_i^n (O_i - P_i)^2}{\sum_i^n (O_i - \bar{O})^2} \quad (17)$$

Where $\bar{O}$ represents the mean of calculated values. The range of E lies between 1.0 (perfect fit) and $-\infty$.

7. CONCLUSIONS

In this study numerical analysis for prediction of depth-averaged velocity for compound channel with converging flood plain using ANN were presented. In the first part of the paper, a 3D model of turbulence stream pattern in compound channel with converging flood plains were simulated using a numerical model. Using experimental and numerical analysis, variation of velocity components for compound channel with converging flood plains were studied. The other part of this paper dealt with the prediction of the depth-averaged velocity field using ANN. In the prediction part, at first, BPNN neural networks were created. Then coordinates of different points were applied as input values and corresponding velocity as target outputs to create ANNs. Some experimental data were used to train the ANNs and some experimental data were used to test the trained ANNs based on BPNN techniques. Finally, the results of ANN and CES methods were compared in sections. The main conclusions of this study are as follows:

1. ANSYS shows a good conformity with the experimental results for predicting the depth-averaged velocity.

2. Results of numerical model showed that the CES was not in good agreement with experimental results for predicting the depth-averaged velocity. Since the one dimensional model of CES is incompetent when it comes to more realistic results.

3. Results of ANNs that had been trained using BPNN indicated that the velocity field was predicted with good approximation in both training and testing methods and it was concluded that the proposed procedures are useful for velocity prediction in non-prismatic compound channel with converging flood plain.

4. Different error analyses are performed to test the strength of the present ANN model. It is found that MAE as 0.033,MAPE as 3.29 which less than 10%,MSE as 0.0004, RMSE as 0.02, E as 0.0.95, R^2 as 0.99 where as CES gave MAE as 0.2, MAPE as 20, MSE as 0.008, RMSE as 0.08, E as 0.75, R^2 as 0.7.

5. The main advantage of ANN is the prediction of the approximate velocity at points where experimental data are not available. In addition, the presented procedure can be used in predicting some other properties of flow besides velocity, such as shear stresses, depth of water or variations of channel bed. In addition, the presented procedure can be applied to prediction and analysis of the properties of other types of channels and other structures across the flow.

Turbulence studies can also be carried out on the same guidelines indicating the turbulent shearing through Reynolds stresses, secondary flow structures, and the turbulent kinetic energy, which can significantly indicate the momentum exchange process and mass transfer due to differential velocity due to two different stages. Overall studies consider only depth averaged streamwise velocity prediction only, since the applicability of numerical modelling is corroborated on the converging compound channel. Since the validation and error analysis shows an undisputable results, which suggestively indicate the application of the numerical method for further studies such as turbulence studies.

8. ACKNOWLEDGEMENTS

The author wish to acknowledge the support from the Institute and the UGC UKIERI Research project (ref no UGC-2013 14/017) by the second authors for carrying out the research work in the Hydraulics Laboratory at National Institute of Technology, Rourkela.

9. REFERENCES

1. Abdeen, M. A. M. (2008). Predicting the impact of vegetations in open channels with different distributaries' operations on water surface profile using artificial neural networks. Journal of Mechanical Science and Technology, 22, 1830–1842.
2. Bhattacharya,B. & Solomatine, D. P. (2005). Neural networks and M5 model trees in modelling water level–discharge relationship. Neurocomputing, 63, 381–396.
3. Bilgil, A., Altun, H. (2008). Investigation of flow resistance in smooth open channels using artificial neural networks. Flow Measurement and Instrumentation 19, 404-408.
4. Cater, J. E. and Williams, J. J. R. (2008). Large eddy simulation of a long asymmetric compound open channel.
5. Cheng, C.T., Ou, C.P., Chau, K.W. (2002). Combining a fuzzy optimal model with agenetic algorithm to solve multi-objective rainfall–runoff model calibration. Journal of Hydrology 268, 72–86.
6. Cokljat, D. (1993). Turbulence Models for Non-circular Ducts and Channels. PhD Thesis, City University London.
7. Ervine, D. A., Koopaei K. B. and Sellin R. H. J. (2000). Two Dimensional Solution for Straight and Meandering Over-bank Flows. J. Hydraul. Eng., ASCE, 126 (9), 653-669.
8. Filonovich MS, Azevedo R, Rojas-Solórzano L, Leal, JB (2013). Credibility Analysis of Computational Fluid Dynamic Simulations for Compound Channel Flow. Journal of Hydroinformatics 15(3), 926-938.
9. Gandhi, B.K., Verma, H.K., Abraham, B.(2010). Investigation of Flow Profile in Open Channels using CFD, 8th Intl Conference on Hydraulic Efficiency Measurement, 243-251.
10. Ghosh, S., and Jena, S.B. (1971). Boundary shear stress distribution in open channel compound. Proc. Inst. Civil Eng. 49, 417–430.
11. Ghosh, S., Pratihar, D.K., Maiti, B., Das, P.K. (2010). Optimum design of a two step planar diffuser: A hybrid approach. Engineering Applications of Computational Fluid Mechanics 4(3), 415-424.

12. Hodges, B. R., & Street, R. L. (1999). On simulation of turbulent nonlinear free-surface flows. J. Comp. Phys. 151, 425–457.
13. Hodskinson, A., and R. Ferguson,(1998). Numerical modelling of separated flow in river bends: model testing and experimental investigation of geometric controls on the extent of flow separation at the concave bank. Hydrological Processes, 12, 1323-1338.
14. Hodskinson, A.,(1996). Computational fluid dynamics as a tool for investigating separated flow in river bends. Earth Surface Processes and Landforms,21, 993-1000.
15. Hsu, T. Y., Grega, L. M., Leighton, R. I. and Wei, T. (2000). Turbulent kinetic energy transport in a corner formed by a solid wall and a free surface. J. Fluid Mech. 410, 343-366.
16. Issa, R. I. (1986). Solution of the implicitly discretised fluid flow equations by operator-splitting. Journal of computational physics, 62(1), 40-65.
17. J. Hydraulic Research 46 (4), 445-453.
18. Jain, S. K. (2008).Development of integrated discharge and sediment rating relation using a compound neural network. Journal of Hydrologic Engineering 13, 124–131.
19. Kara, S., Stoesser, T. and Sturm, T. W. (2012). Turbulence statistics in compound channels with deep and shallow overbank flows. J. Hydraulic Research 50 (5), 482-493.
20. Kawahara,Y., & Tamai, N. (1988). Numerical calculation of turbulent flows in compound channels with an algebraic stress turbulence model. In: Proc. 3rd Symp. Refined Flow Modeling and Turbulence Measurements, Tokyo, Japan, pp. 9–17.
21. Khatua K.K, Patra K C, Mohanty, P.K. (2012). Stage Discharge Prediction for Straight and Smooth Compound Channels with Wide Floodplains. J. Hydraul. Eng., ASCE, 138 (1), 93-99.
22. Khatua, K.K., Patra, K.C. (2008). Boundary Shear Stress Distribution in Compound Open Channel Flow. J. Hydraul. Eng., ISH, 12 (3), 39-55.
23. Knight, D. W., Wright, N. G. and Morvan, H. P. (2005) .Guidelines for applying commercial CFD software
24. Krishnappan,B. G., and Lau, Y. L. 1986. Turbulence modelling of flood plain flows. J. Hydraulic Eng., ASCE, 112(4), 251-266.
25. Lane S. N., Bradbrook, K. F., Richards, K. S., Biron, P. A. & Roy, A. G. (1999). The application of computational fluid dynamics to natural river channels: three-dimensional versus two dimensional approaches. Geomorphology 29, 1–20.
26. Lin, J.Y., Cheng, C.T., Chau, K.W. (2006). Using support vector machines for long-term discharge prediction. Hydrological Sciences Journal 51(4): 599-612.
27. Menter, F. R. (1994) .Two-equation eddy-viscosity turbulence models for engineering applications. AIAA, 32 (8), 1598 – 1605.
28. Morvan, H. P.(2001). Three-dimensional Simulation of River Flood Flows. PhD Thesis,University of Glasgow, Glasgow.
29. Muzzammil, M. (2008). Application of neural networks to scour depth prediction at the bridge abutments. Engineering Applications of Computational Fluid Mechanics 2(1), 30-40.
30. Myers,W. R. C., and Elsawy (1975). Boundary Shear in Channel with Floodplain. J. Hydraul. Eng., ASCE, 101(HY7), 933-946.
31. Nakayama, A. & Yokojima, S. (2002). LES of open-channel flow with free-surface fluctuations. In: Proc. Hydraul. Eng. JSCE. 46, 373–378.

32. NASH, J. E., SUTCLIFFE, J. V.(1970). River flow forecasting through conceptual models, Part I. A discussion of principles.J. Hydrol. 10, 282–290.
33. Pan, Y., & Banerjee, S. (1995). Numerical investigation of free-surface turbulence in open-channel flows. Phys. Fluids ,113 (7),1649–1664.
34. Rezaei, B.(2006). Overbank flow in compound channels with prismatic and non-prismatic floodplains. PhD Thesis. Univ. of Birmingham. U.K.
35. Rhodes, D. G., and Knight, D. W. (1994). Distribution of Shear Force on Boundary of Smooth Rectangular Duct. Journal of Hydralic Engg., 120-7, 787– 807.
36. Safikhani, H., Khalkhali, A., Farajpoor, M. (2011). Pareto Based Multi-Objective Optimization of Centrifugal Pumps Using CFD, Neural Networks and Genetic Algorithms. Engineering Applications of Computational Fluid Mechanics 5(1), 37-48.
37. Sahu, M., Khatua, K. K. & Mahapatra, S. S. (2011). A neural network approach for prediction of discharge in straight compound open channel flow. Flow Measurement and Instrumentation, 22, 438–446.
38. Shiono, K., Knight, D. W. (1988). Refined Modelling and Turbulance Measurements. Proceedings of 3rd International Symposium, IAHR, Tokyo, Japan, July, 26-28.
39. Sinha, S. K., Sotiropoulos, F. & Odgaard, A. J.(1998). Three dimensional numerical model for flow through natural rivers.J. Hydraul. Eng. 124(1), 13–24.
40. Spalding, D. B. (1980) .Genmix: a general computer program for two-dimensional parabolic phenomena, Pergamon Press, Oxford.
41. Speziale, C. G., Sarkar, S. and Gatski, T. B. (1991) .Modelling the pressure-strain correlation of turbulence: an invariant dynamical systems approach. J. Fluid Mech. 277, 245-272.
42. Thomas, T. G. and Williams, J. J. R. (1995a). Large eddy simulation of turbulent flow in an asymmetric compound channel. J. Hydraulic Research 33 (1), 27-41.
43. to open channel flow. Report based on the research work conducted under EPSRC Grants GR/R43716/01 and GR/R43723/01.
44. Unal, B., Mamak, M., Seckin, G. & Cobaner, M. (2010). Comparison of an ANN approach with 1-D and 2-D methods for estimating discharge capacity of straight compound channels. Advances in Engineering Software, 41, 120–129.
45. Van Hooff, T., & Blocken, B. (2010). Coupled urban wind flow and indoor natural ventilation modelling on a high-resolution grid: A case study for the Amsterdam ArenA stadium. Environmental Modelling & Software, 25(1), 51-65.
46. Van Hooff, T., and Bert Blocken. "Coupled urban wind flow and indoor natural ventilation modelling on a high-resolution grid: A case study for the Amsterdam ArenA stadium." Environmental Modelling & Software 25.1 (2010): 51-65.
47. Wang, W.C., Chau, K.W., Cheng, C,T., Qiu, L. (2009).A comparison of performance of several artificial intelligence methods for forecasting monthly discharge time series. Journal of Hydrology 374, 294-306.
48. Wilcox, D. C. 1988. Reassessment of the scale-determining equation for advanced turbulence models. AIAA, 26, 1299–1310.
49. Wu, C.L., Chau, K.W., Li, Y.S. (2009). Predicting monthly streamflow using data-driven models coupled with data-preprocessing techniques.Water Resources Research 45, 1-23.
50. Xie, Z., Lin, B. and Falconer, R. A. (2013). Large-eddy simulation of the turbulent structure in compound open-channel flows. Advances in Water Resources 53, 66-75.

51. Yuhong, Z., Wenxin, H. (2009). Application of artificial neural network to predict the friction factor of open channel flow. Communications in Nonlinear Science and Numerical Simulation 14, 2373-2378.

Table1. Hydraulic parameters for the experimental channel data

Sl. No	Item Description	Converging Compound Channel
1	Geometry of main channel	Rectangular
2	Geometry of flood plain	Converging
3	Main channel width (b)	0.5m
4	Bank full depth of main channel	0.1m
5	Top width of compound channel (B1)	before convergence 0.9m
6	Top width of compound channel (B2)	after convergence 0.5m
7	Converging length of the channels	0.84m, 1.26, 2.26m
8	Slope of the channel	0.0011
9	Angle of convergence of flood plain ($^{\theta}$)	12.38,9, 5
10	Position of experimental section 1	start of the converging part
11	Position of experimental section 2	Middle of converging part
12	Position of experimental section	end of converging part.

Table 2. Values of the constants in the k- ω model (Wilcox 1988)

β'	β	α	σ_k	σ_ω
0.09	0.075	5/9	2	2

Table 3.Input and output data used for the present analysis

Sl.No	Converging angles	Flood plain type	Converging Length
1	1.91	Convergent	6m
2	3.81	Convergent	6m
3	11.31	Convergent	2m
4	5	Convergent	2.26m
5	9	Convergent	1.28m
6	12.38	Convergent	0.84m
8	2.5	Convergent	4.58
9	3	Convergent	3.82
10	4	Convergent	2.86
11	7	Convergent	1.64
12	10	Convergent	1.15
13	14	Convergent	0.8
14	15	Convergent	0.77

15	17	Convergent	0.68
16	20	Convergent	0.58

Table 4 Different Error Analysis

	ANN	CES
MSE	0.0004	0.008
RMSE	0.02	0.08
MAE	0.033	0.2
MAPE	3.29	20
E	0.95	0.70
R^2	0.99	0.75

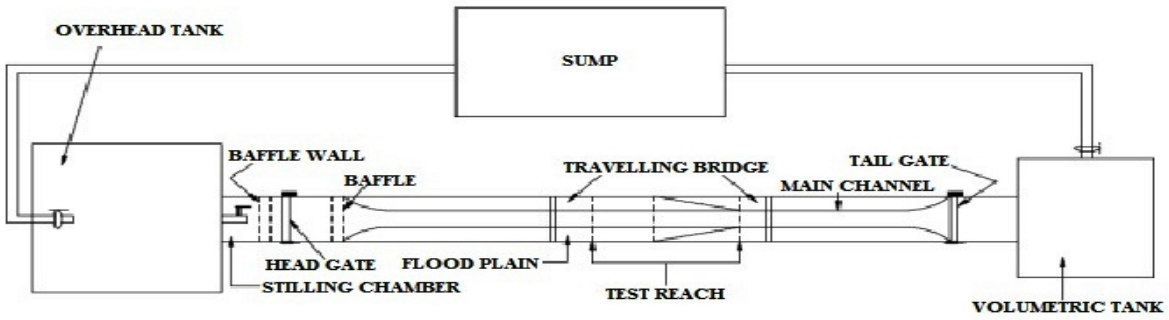

Figure 1(a). Plan view of Experimental Setup

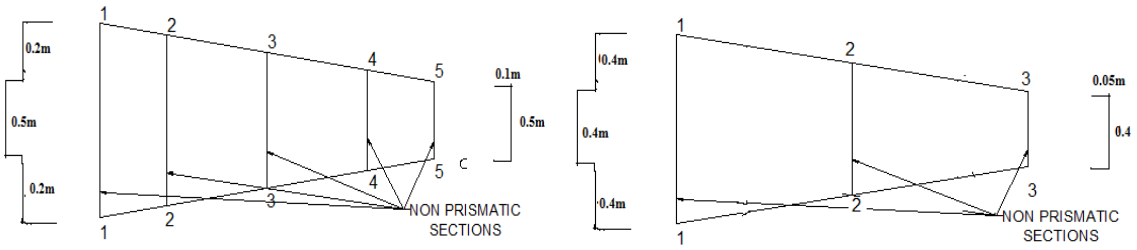

Figure 1(b). Plan view of different test reaches with cross-sectional dimensions of non-prismatic compound channel from both NITR & Rezaei (2006) channels

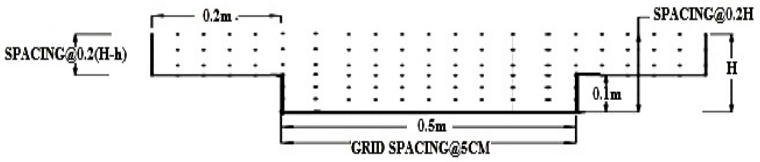

Figure 1(c). Typical grid showing the arrangement of velocity measurement points at the test sections (1-1,2-2,3-3,4-4 &5-5)

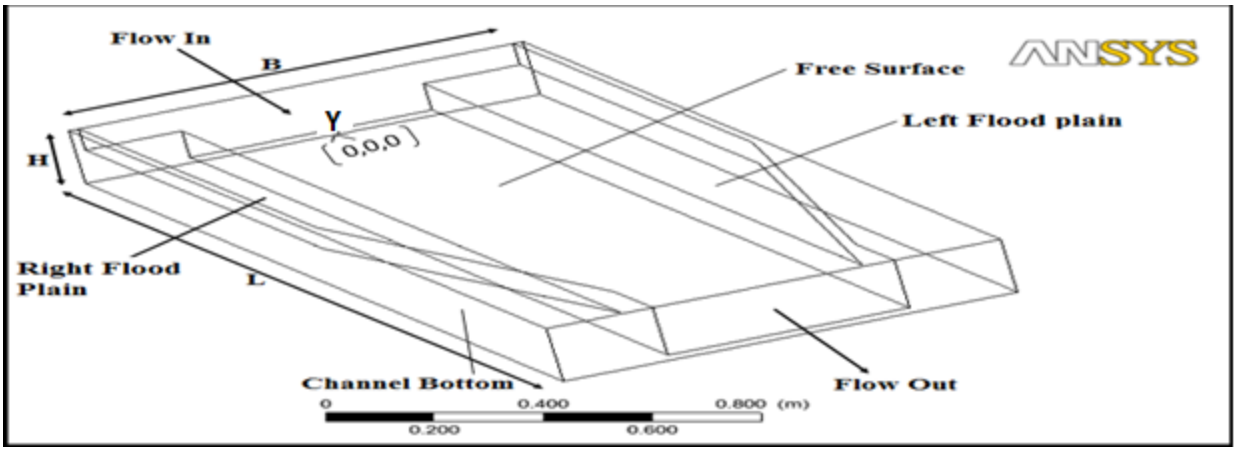

2. Geometry Setup of a Compound Channel with converging flood plains

-

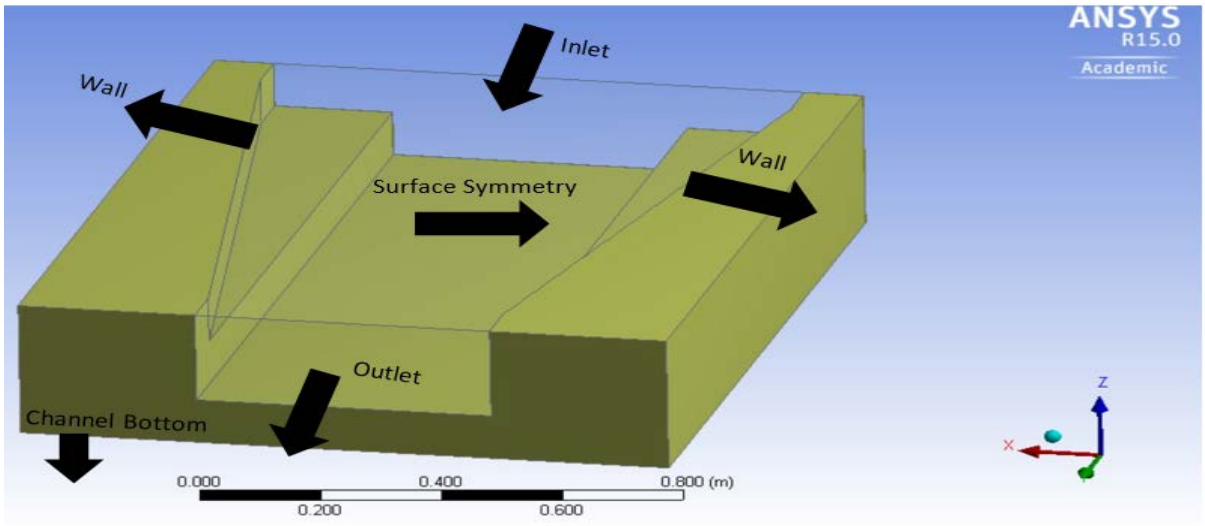

3. Different Geometrical entities used in a compound channel with converging flood plain

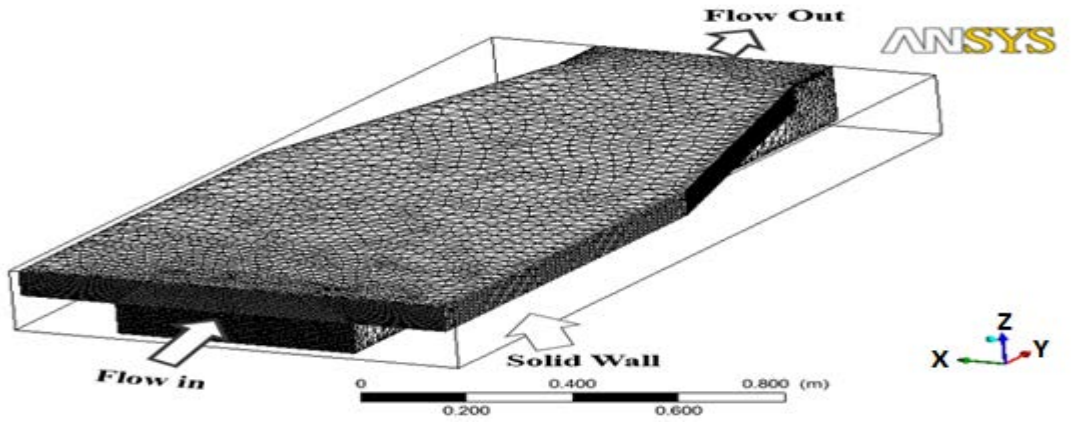

4. A schematic view of the Grid used in the Numerical Model

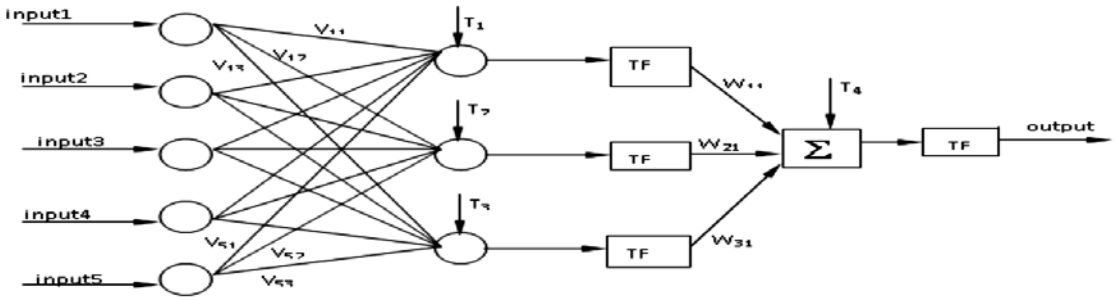

Fig.5.The architecture of back propagation neural network model

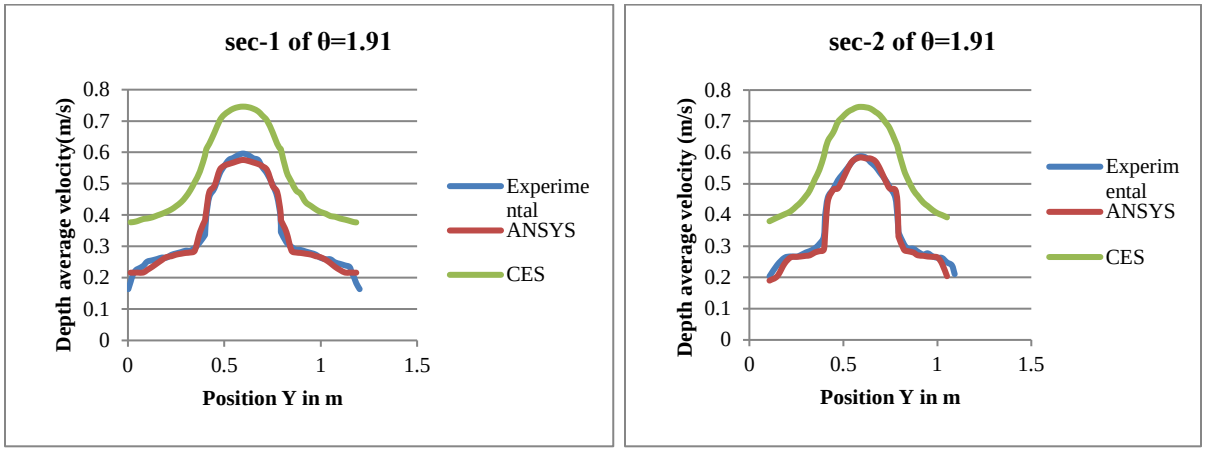

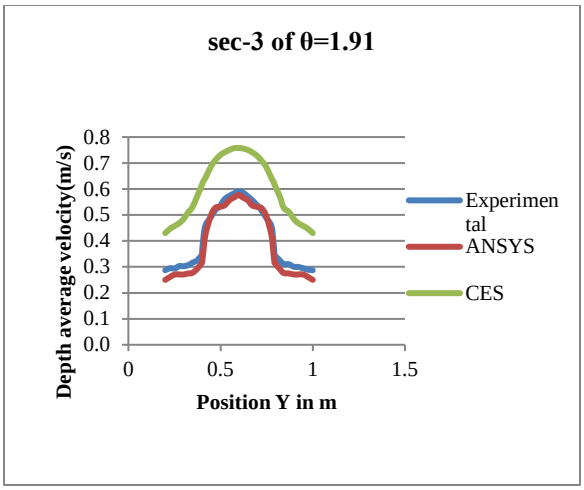

Figure 6 (a) , (b) , (c) Depth-averaged velocity of Sec 1, Sec 2 , Sec 3 of $\theta=1.91^0$

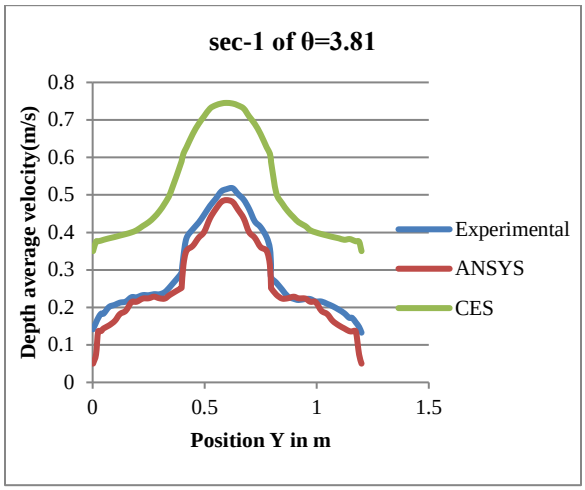

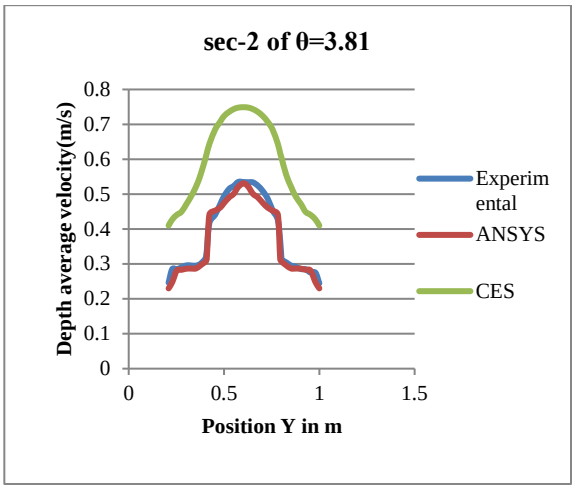

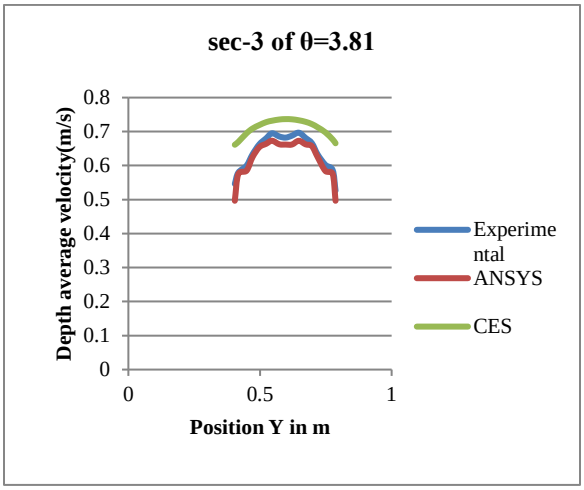

Figure 7 (a) , (b) , (c) Depth-averaged velocity of Sec 1, Sec 2 , Sec 3 of $\theta=3.81^0$

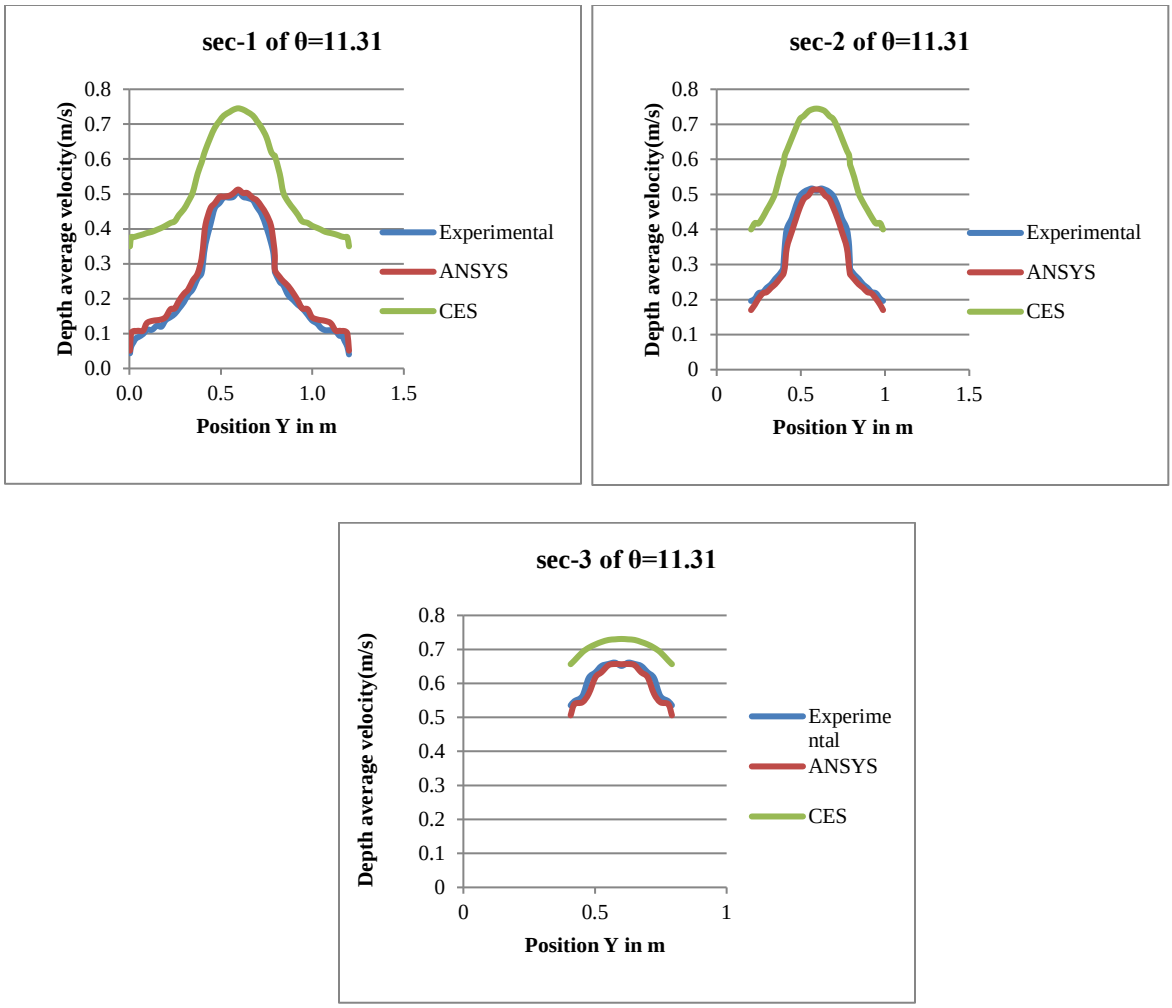

Figure 8 (a) , (b) , (c) Depth-averaged velocity of Sec 1, Sec 2 , Sec 3 of $\theta=11.31^0$

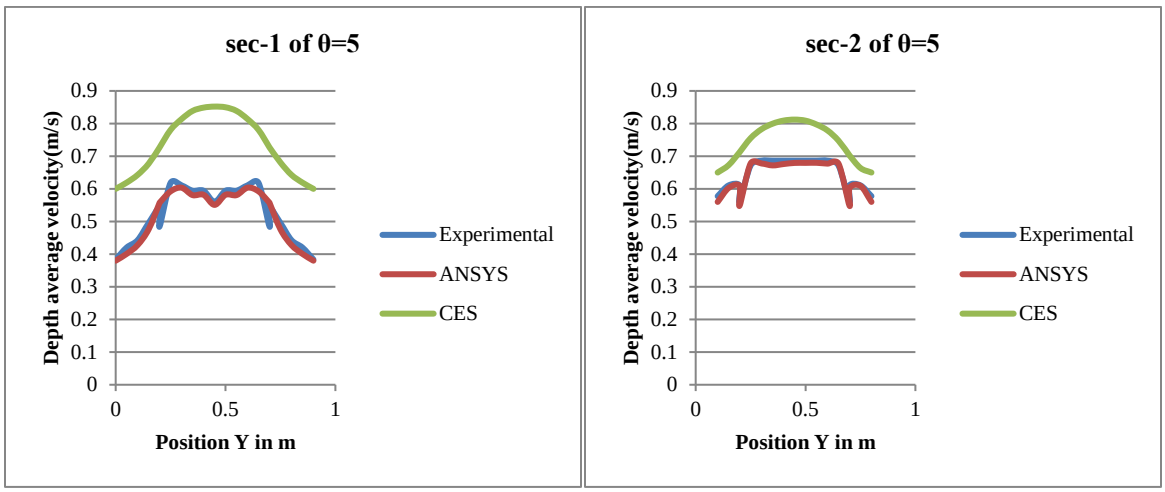

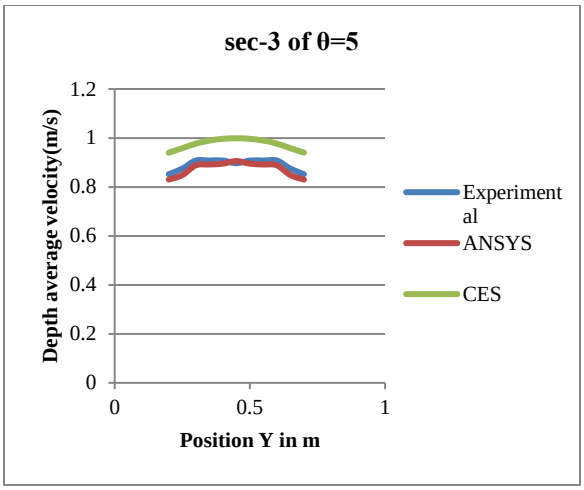

Figure 9 (a) , (b) , (c) Depth-averaged velocity of Sec 1, Sec 2 , Sec 3 of $\theta = 5^0$

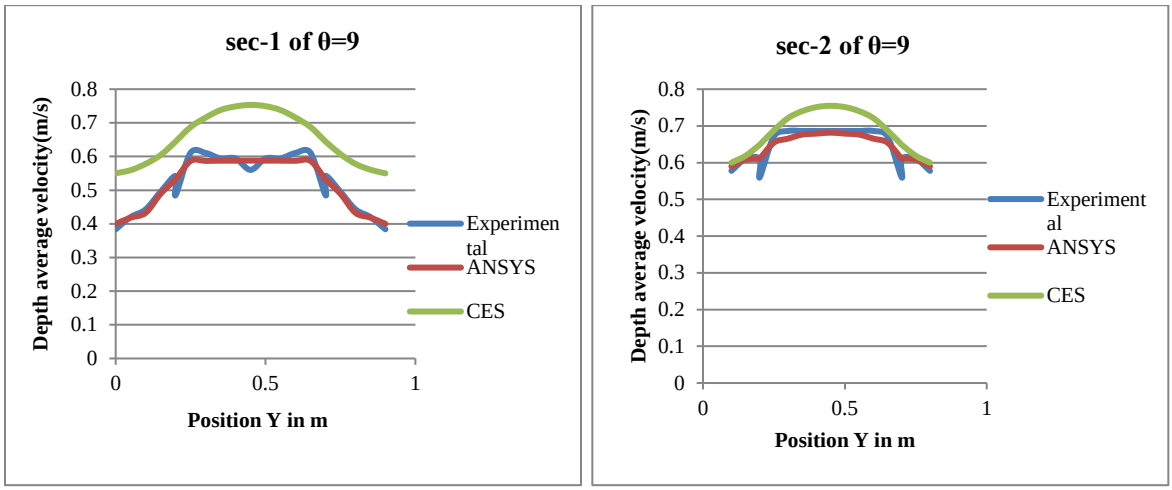

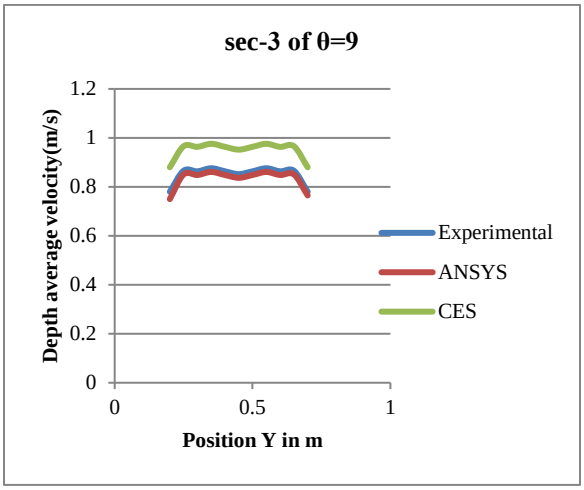

Figure 10 (a) , (b) , (c) Depth-averaged velocity of Sec 1, Sec 2 , Sec 3 of $\theta = 9^0$

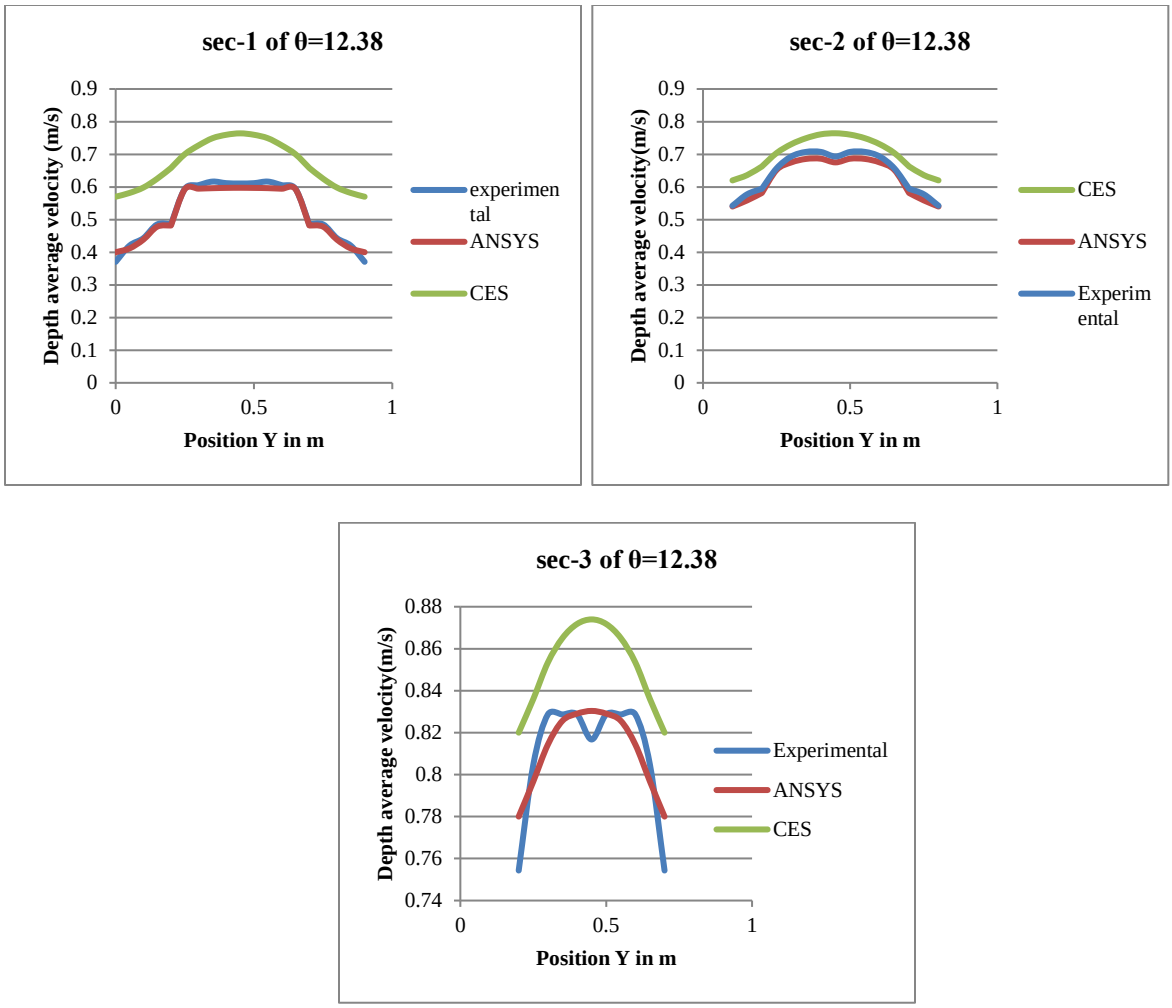

Figure 11 (a) , (b) , (c) Depth-averaged velocity of Sec 1, Sec 2 , Sec 3 of θ =12.38^0

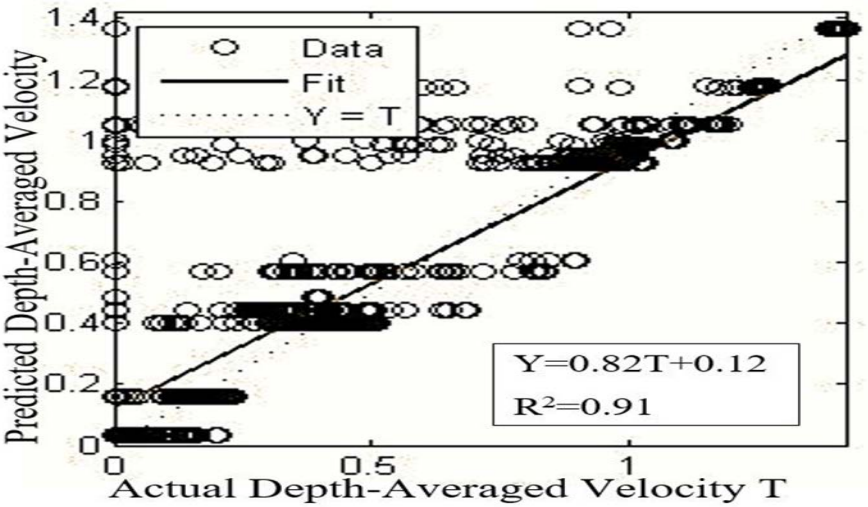

Fig 13 Correlation plot of actual depth-averaged velocity and predicted depth-averaged velocity

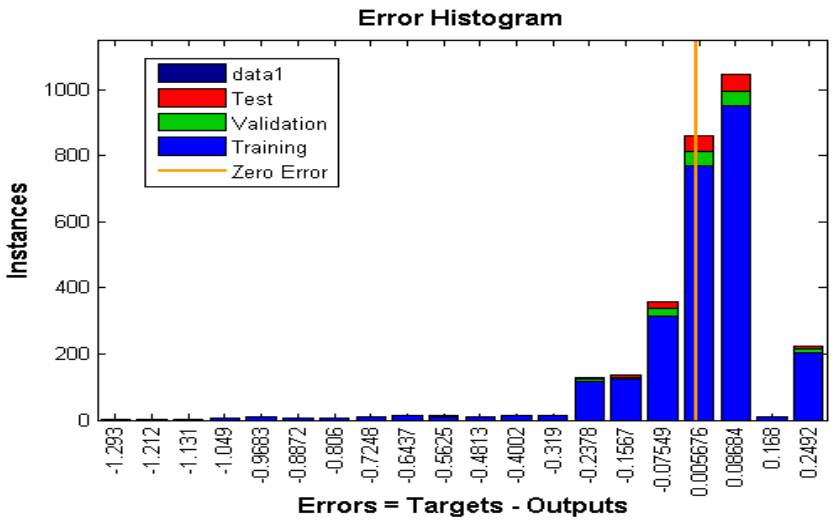

Fig 14 Error Histogram